

Quasi-fractionalization of spin in a cluster-based Haldane state supported by chirality of a triangular spin tube

Takanori Sugimoto* and Takami Tohyama

Department of Applied Physics, Tokyo University of Science, Katsushika, Tokyo 125-8585, Japan

(Dated: August 3, 2021)

Fractionalization of quantum degrees of freedom holds the key to finding new phenomena in physics, e.g., the quark model in hadron physics, the spin-charge separation in strongly-correlated electron systems, and the fractional quantum Hall effect. A typical example of the fractionalization in quantum spin systems is the spin-1 Haldane state, whose intriguing characteristics are well described by fractionalized $S = 1/2$ virtual spins in a bilinear-biquadratic spin-1 chain, the so-called Affleck–Kennedy–Lieb–Tasaki model, delivering two individual spin-1/2 degrees of freedom as edge states. Here we theoretically propose an exotic extension of the Haldane state and chirality in a triangular spin tube, inducing a *quasi*-fractionalization of spin-1/2 degree of freedom, i.e., a *quarter* spin. Existence of the edge state is confirmed both analytically and numerically, combining a low-energy perturbation theory and variational matrix-product state method. Our study can not only propose a new quantum spin property but pave a way to novel quantum states of matter.

PACS numbers: Valid PACS appear here

Historically, developments of physics have often been supported by discoveries of new fractionalization mechanism and derivative hidden degrees of freedom. Elementary particles in the standard model are the fruits of fractionalization, and moreover, there still remain some fractionalized particles, e.g., a magnetic monopole [1, 2] and an axion [3, 4], in the dark. The concept of fractionalization also plays a key role in condensed-matter physics, leading to discoveries of the spin-charge separation in strongly-correlated electron systems [5], the fractional quantum Hall effect [6, 7], and the Majorana fermion in topological superconductors [8]. Furthermore, as quantum spin counterparts, intensive studies have been performed on the Haldane state in a spin-1 chain [9, 10] and the Kitaev model with anisotropic spin interactions [11] so far. Particularly, the Haldane state has been used to demonstrate exotic phenomena, symmetry-protected topological phase [12–15] and holographic quantum computing [16–20], thanks to its simplicity of both analytical and numerical calculations.

Main characteristics in the Haldane state, which is the ground state in an $S = 1$ antiferromagnetic spin chain, are clearly explained in the bilinear-biquadratic spin-1 chain, the so-called Affleck–Kennedy–Lieb–Tasaki (AKLT) model [21]. In the AKLT model, an $S = 1$ spin is decomposed into two $S = 1/2$ virtual spins at each site, and neighboring spins connected with inter-site bonds are antisymmetrized reflecting the antiferromagnetism [see Fig. 1(a)]. To restore the $S = 1$ spin, corresponding two spins at each site are symmetrized with a projection operator into an even parity space. Note that in this state, there is a non-trivial topological order defined by a long-ranged string correlation [22–24]. This procedure can be extended into more than two spins at each site, resulting in the cluster-based Haldane state (CBHS) in

a spin cluster chain (SCC) [25–27]. Meanwhile, with the open boundary condition, it is well known that the original Haldane state exhibits two edge states corresponding to spin-1/2 degrees of freedom [see Fig. 1(a)]. Similarly, in the CBHS, there should be the edge states, while the edge site contains many $S = 1/2$ spins. Hence, a naive question arises; if we obtain a way to detect only one of the spins at the edges, how does the spin degree of freedom behave in this state, delivering a new type of fractionalization?

To answer this question, in this letter, we consider a CBHS appearing in a triangular spin tube (TST) coupled with chirality degree of freedom [see Fig. 1(b)]. In this model, the chirality plays the role of an $S = 1/2$ pseudo spin in the low-energy states [28, 29]. If we add a Heisenberg-type coupling between the real and pseudo spins, it can split the four-fold ground-state degeneracy into a triplet and a singlet in a triangle cluster. The triplet state is regarded as an $S = 1$ spin as a result of hybridization of the real and pseudo spins. Thus, introducing antiferromagnetic interactions between neighboring triangles which are much smaller than the intra-cluster interactions induces a CBHS. Since the chirality is not directly coupled with the magnetic field, only the real-spin component at edge site can be controlled with applying the magnetic field.

As a concrete description, we propose the model Hamiltonian of $S = 1/2$ TST as follows,

$$\mathcal{H}_0 = \sum_{j=1}^L \mathcal{H}_J^{(j)} + \sum_{j=1}^L \mathcal{H}_K^{(j)} + \sum_{j=1}^{L-1} \mathcal{H}_{J'}^{(j)} \quad (1)$$

with

$$\mathcal{H}_J^{(j)} = J \sum_{i < i'} \mathbf{S}_{i,j} \cdot \mathbf{S}_{i',j}, \quad \mathcal{H}_K^{(j)} = -K \mathbf{S}_{\text{tot},j} \cdot \boldsymbol{\chi}_j, \quad (2)$$

$$\mathcal{H}_{J'}^{(j)} = J'_1 \sum_i \mathbf{S}_{i,j} \cdot \mathbf{S}_{i,j+1} + J'_2 \sum_{i \neq i'} \mathbf{S}_{i,j} \cdot \mathbf{S}_{i',j+1}, \quad (3)$$

* sugimoto.takanori@rs.tus.ac.jp

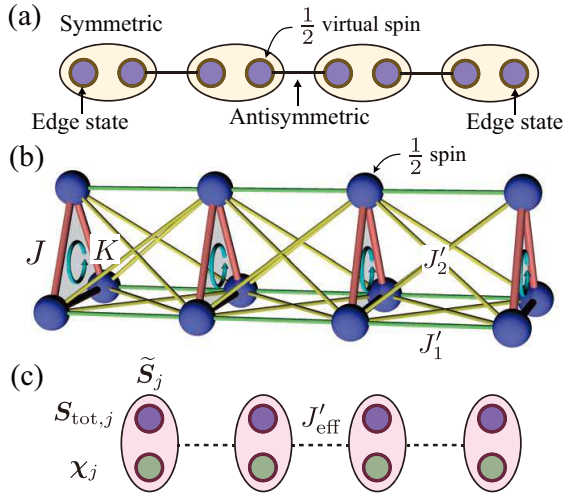


FIG. 1. (a) Schematic ground state of the AKLT model. An $S = 1$ spin is decomposed into two $S = 1/2$ virtual spins (two blue balls in an orange oval). The orange oval (black solid line) represents symmetric (antisymmetric) configuration. As edge states, there are spin-1/2 degrees of freedom disconnected from solid bond with open boundary condition. (b) An $S = 1/2$ TST. Blue balls denote $S = 1/2$ spins. Red, green, and yellow bonds represent J , J'_1 , and J'_2 interactions in (A2) and (A3), where the K term is shown as a cyan circular arrow. (c) Low-energy effective model of (A1), corresponding to (9) with $J'_1 = J'_2$. Blue (green) balls represent spin-1/2 degrees of freedom corresponding to $\mathbf{S}_{\text{tot},j}$ (χ_j). Pink oval represents a spin-1 degree of freedom ($\tilde{\mathbf{S}}_j$) given by symmetrization of $\mathbf{S}_{\text{tot},j}$ and χ_j . Dashed line denotes the effective antiferromagnetic exchange interaction $J'_{\text{eff}} = J'_1$.

where L is the number of clusters. The local Hamiltonians, $\mathcal{H}_J^{(j)}$, $\mathcal{H}_K^{(j)}$, and $\mathcal{H}_{J'}^{(j)}$, represent intra-cluster spin interactions of the j -th cluster, a spin-chirality interaction of the j -th cluster, and inter-cluster spin interactions between the j -th and $(j+1)$ -th clusters, respectively. The $S = 1/2$ local spin (the total spin) operator in a cluster is denoted by $\mathbf{S}_{i,j}$ ($\mathbf{S}_{\text{tot},j} = \sum_i \mathbf{S}_{i,j}$), where $i = 1, 2, 3$ ($j = 1, 2, \dots, L$) denotes the site (cluster) index. The $S = 1/2$ pseudo spin operator corresponding to the scalar chirality is represented by χ_j as explained below. In this model, we consider antiferromagnetic Heisenberg interactions $J > 0$ and $J'_k > 0$ ($k = 1, 2$), and a ferromagnetic Heisenberg-type interaction between $\mathbf{S}_{\text{tot},j}$ and χ_j ($K > 0$). As the SCC condition, we assume that the inter-cluster interactions J'_k ($k = 1, 2$) are much smaller than the intra-cluster interactions J and K . It is worthfully noted that intensive studies on TSTs have been performed both theoretically [28–40] and experimentally [41–46], while to the best of our knowledge, the spin-chirality interaction has not been considered so far. Realizability of this interaction is discussed below.

To obtain an effective model based on low-energy perturbation theory, we start with the intra-cluster Hamiltonians (A2), shown in Fig. 2(a), because of the SCC condition $J'_k \ll J, K$. Without the K term, the local

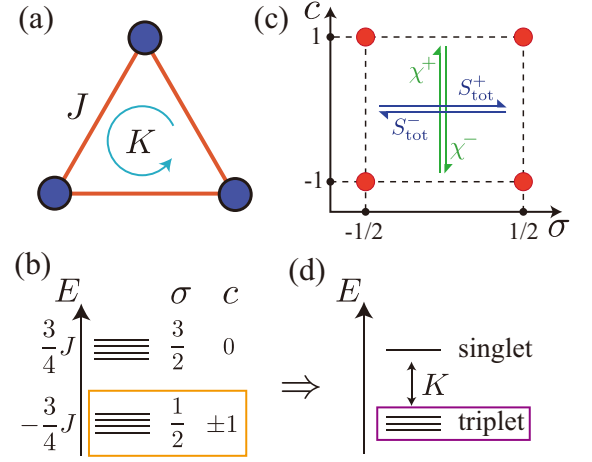


FIG. 2. (a) A triangle spin cluster. The J and K terms in (A2) are denoted by red bond and cyan circular arrow, respectively. (b) Energy spectrum of the triangle cluster with $K = 0$, where σ and c represent the eigenvalues of $S_{\text{tot},j}^z$ and χ_j , respectively. There are two quartets. (c) Eigenstates (red balls) of the lower quartet (orange region) in (b) and ladder operators of $\mathbf{S}_{\text{tot},j}$ and χ_j . (d) Introducing a finite $K > 0$, the lower quartet splits to a singlet and a triplet. The triplet (purple region) is regarded as an $S = 1$ pseudo spin.

Hamiltonian corresponds to a uniform antiferromagnetic Heisenberg model on a triangle cluster. The eigenstates are decomposed into a quartet of $S_{\text{tot},j} = 3/2$ and degenerate two doublets of $S_{\text{tot},j} = 1/2$ in Fig. 2(b). All the local eigenstates $|\sigma, c\rangle$ are classified by z component of the total spin operator $S_{\text{tot},j}^z$ and the scalar chirality operator $\chi_j \equiv (4/\sqrt{3})\mathbf{S}_{1,j} \cdot \mathbf{S}_{2,j} \times \mathbf{S}_{3,j}$, where σ (c) is the eigenvalue of $S_{\text{tot},j}^z$ (χ_j), because of the commutation relations, $[\mathcal{H}_J^{(j)}, S_{\text{tot},j}^z] = [\mathcal{H}_J^{(j)}, \chi_j] = [S_{\text{tot},j}^z, \chi_j] = 0$:

$$|\pm \frac{3}{2}, 0\rangle_j = |\pm \pm \pm\rangle_j, \quad (4)$$

$$|\pm \frac{1}{2}, 0\rangle_j = \frac{\pm 1}{\sqrt{3}} \left(|\pm \pm \mp\rangle_j + |\pm \mp \pm\rangle_j + |\mp \pm \pm\rangle_j \right), \quad (5)$$

$$|\pm \frac{1}{2}, 1\rangle_j = \frac{\pm 1}{\sqrt{3}} \left(e^{-i\phi} |\pm \pm \mp\rangle_j + e^{i\phi} |\pm \mp \pm\rangle_j + |\mp \pm \pm\rangle_j \right), \quad (6)$$

$$|\pm \frac{1}{2}, -1\rangle_j = \frac{\pm 1}{\sqrt{3}} \left(e^{i\phi} |\pm \pm \mp\rangle_j + e^{-i\phi} |\pm \mp \pm\rangle_j + |\mp \pm \pm\rangle_j \right), \quad (7)$$

with $\phi = 2\pi/3$ and the imaginary unit $i = \sqrt{-1}$. The ket states in the right-hand side denote the direct products of one-spin eigenstate, e.g., $|+-+\rangle_j = |\uparrow\rangle_{1,j} |\downarrow\rangle_{2,j} |\uparrow\rangle_{3,j}$. Figure 2(c) shows the lower quartet [orange region in Fig. 2(b)] in the parameter space of σ and c . In the same manner as $S = 1/2$ spin operators, we can construct a pseudo spin operator χ_j with $\chi_j^z \equiv \chi_j/2$ and corresponding ladder operators, $\chi_j^\pm \equiv \sum_{\sigma=\pm\frac{1}{2}} |\sigma, \pm 1\rangle_j \langle \sigma, \mp 1|_j$. Hence, the x and y components of the pseudo spin

operator are given by $\chi_j^x \equiv (\chi_j^+ + \chi_j^-)/2$ and $\chi_j^y \equiv (\chi_j^+ - \chi_j^-)/(2i)$, respectively. Introducing a finite $K > 0$ with the pseudo spin operator χ_j in $\mathcal{H}_K^{(j)}$, we can obtain a triplet $|\widetilde{m}\rangle_j$ ($m = 0, \pm 1$) as local ground states [see Fig. 2(d)] given by,

$$|\widetilde{\pm 1}\rangle_j = |\pm \frac{1}{2}, \pm 1\rangle_j, \quad |\widetilde{0}\rangle_j = \frac{1}{\sqrt{2}} \left(|\frac{1}{2}, -1\rangle_j + |-\frac{1}{2}, 1\rangle_j \right), \quad (8)$$

where m corresponds to the eigenvalue of $\widetilde{S}_j^z = S_{\text{tot},j}^z + \chi_j^z$.

$$\mathcal{H}_{\text{eff}} = \sum_j \left\{ \left[\left(\frac{5}{3}J'_1 - \frac{2}{3}J'_2 \right) \widetilde{S}_j^z \widetilde{S}_{j+1}^z + J'_1 \left(\widetilde{S}_j^x \widetilde{S}_{j+1}^x + \widetilde{S}_j^y \widetilde{S}_{j+1}^y \right) \right] + \frac{8}{3}(J'_1 - J'_2) \left(\frac{1}{2} \widetilde{S}_j^z \widetilde{S}_{j+1}^z + \widetilde{S}_j^x \widetilde{S}_{j+1}^x + \widetilde{S}_j^y \widetilde{S}_{j+1}^y \right)^2 - \frac{2}{3}(J'_1 - J'_2) \left[2 - (\widetilde{S}_j^z)^2 \right] \left[2 - (\widetilde{S}_{j+1}^z)^2 \right] \right\} + \text{const.} \quad (9)$$

In the effective Hamiltonian, there are an anisotropic exchange interaction, an anisotropic biquadratic interaction, and an additional term favoring zero magnetization. Assuming $J'_1 = J'_2$, the effective Hamiltonian is equivalent to a Heisenberg chain of the $S = 1$ pseudo spins. Therefore, the ground state of the SCC Hamiltonian (A1) is a CBHS consisting of the $S = 1$ pseudo spins with $J'_1 = J'_2$.

To confirm this statement, we have performed numerical calculations for TST (A1) by the variational matrix-product state method [47] (see Appendix B). In the calculations, we have obtained several expectation values and correlation functions in addition to eigenstates and eigen-energies. We have checked the sufficient convergence (the truncation error $\epsilon_{\text{trunc}} \lesssim 10^{-6}$) for the bond dimension $D \geq 300$. As the parameters of Hamiltonians, we choose $J'_1 = J'_2 = J/(10\sqrt{2})$ and $K = J/2$ for the results in Fig. 3.

Firstly, we show pseudo spin and string correlation functions [22–24] defined by,

$$C_{\text{spn}}(r) = \left\langle \widetilde{S}_j^z \widetilde{S}_{j+r}^z \right\rangle, \quad (10)$$

$$C_{\text{str}}(r) = \left\langle \widetilde{S}_j^z \exp \left(i\pi \sum_{k=j+1}^{j+r-1} \widetilde{S}_k^z \right) \widetilde{S}_{j+r}^z \right\rangle. \quad (11)$$

For the numerical calculation, we have chosen $j = L/2 - \lfloor r/2 \rfloor$, where the floor function $\lfloor x \rfloor$ represents the integer part of x . Figure 3(a) shows the correlation functions at the ground state in an $L = 120$ TST (A1). We can see convergence of the string correlation to a finite constant irrespective to the exponential decay of the spin correlation, indicating the (cluster-based) Haldane state.

Next, we check existence of edge states in $\widetilde{M} =$

Note that the K term does not affect the upper quartet, because the eigenvalue of the chirality is zero ($c = 0$) in the upper quartet.

At low temperatures $T \lesssim K$, only the local triplet states $|\widetilde{m}\rangle_j$ are relevant to low-energy physics with small enough inter-cluster interactions. This corresponds to the $S = 1$ pseudo spin, $\widetilde{\mathcal{S}}_j \equiv \mathcal{P}_j(S_{\text{tot},j}^z + \chi_j^z)\mathcal{P}_j$ with a projection operator $\mathcal{P}_j = \sum_m |\widetilde{m}\rangle_j \langle \widetilde{m}|_j$. Moreover, we can obtain an effective Hamiltonian of the pseudo spin-1 operator (see Appendix A for the derivation) as follows,

$\sum_j \langle \widetilde{S}_j^z \rangle = 1$ eigenstate, which is the first excited state with an energy gap converging to zero in the thermodynamical limit $\Delta_1 \xrightarrow{L \rightarrow \infty} 0$. In Fig. 3(b), two expectation values in absolute value are shown: $|\langle S_{\text{tot},j}^z \rangle|$ in an $L = 120$ TST and for comparison, $|\langle S_j^z \rangle|$ in an $N = 120$ spin-1 chain, where N is the number of spins, exhibiting edge states in the Haldane state. The pseudo spin's edge states in the TST are localized and decoupled at two edges as well as the edge states of the Haldane state. The real-spin component $\langle S_{\text{tot},j}^z \rangle$ is similarly distributed, while the absolute value is almost the half of the spin $|\langle S_j^z \rangle|$ in the Haldane state. The edge state in the original Haldane state has the magnitude of $S = 1/2$ spin, so that the real-spin component $\langle S_{\text{tot},j}^z \rangle$ in the TST can be regarded as a half of the $S = 1/2$ spin, i.e., a *quarter* ($S = 1/4$) spin. It is not the case that the real-spin component does neither obey any new algebra nor have any new group of an $S = 1/4$ spin, but rather the case that the magnitude is almost equivalent to a half of $S = 1/2$ spin.

Moreover, to confirm stability of the edge states, we examine response to two types of external fields given by,

$$\mathcal{H}_Z = -h_z \sum_j S_{\text{tot},j}^z, \quad \widetilde{\mathcal{H}}_Z = -\widetilde{h}_z \sum_j (S_{\text{tot},j}^z + \chi_j^z). \quad (12)$$

The former (latter) Hamiltonian is the Zeeman term of real (pseudo) spins. Note that the TST Hamiltonian (A1) does not commute with the former term, but the latter term, because the Heisenberg-type interaction of the real spin and chirality $\mathbf{S}_{\text{tot},j} \cdot \chi$ in $\mathcal{H}_K^{(j)}$ breaks the conservation law of total spin and keeps the sum of total spin and chirality. Therefore, instead of the real magnetization

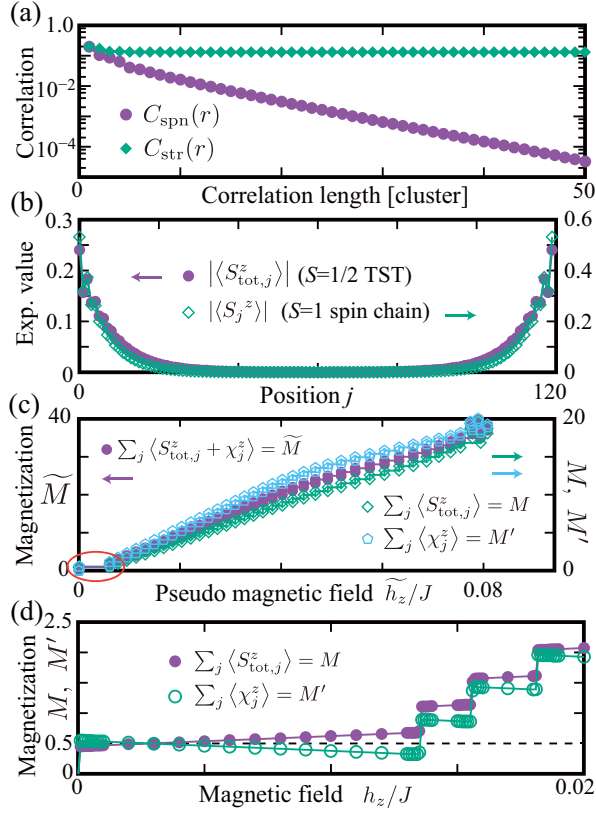


FIG. 3. (a) Pseudo spin and string correlation functions $C_{\text{spn}}(r)$ and $C_{\text{str}}(r)$ at the $\tilde{M} = 0$ ground state in an $L = 120$ ($D = 500$) TST. (b) Local absolute expectation value of the real spin $|\langle S_{\text{tot},j}^z \rangle|$ at the $\tilde{M} = 1$ eigenstate in an $L = 120$ ($D = 500$) TST. For comparison, expectation value of spin $|\langle S_j^z \rangle|$ is shown at $M = 1$ in an $N = 120$ ($D = 300$) spin-1 chain. (c) (Pseudo) magnetization \tilde{M} , M' , and M curves with applied pseudo magnetic field \tilde{h}_z in an $L = 40$ ($D = 300$) TST. Red oval denotes a magnetization plateau at $\tilde{M} = 1$. (d) Response of expectation values of the real and pseudo spins $\sum_j \langle S_{\text{tot},j}^z \rangle$ and $\sum_j \langle \chi_j^z \rangle$ to real magnetic field h_z in an $L = 60$ ($D = 300$) TST. The dashed line denotes the M ($M' = 0.5$) level.

$M = \sum_j \langle S_{\text{tot},j}^z \rangle$, pseudo magnetization $\tilde{M} = \sum_j \langle \tilde{S}_j^z \rangle$ is a good quantum number. Figure 3(c) presents the pseudo magnetization curves with applied the pseudo magnetic field \tilde{h}_z , whereas the real magnetization and chirality versus the real magnetic field h_z are shown in Fig. 3(d). In the pseudo magnetization [Fig. 3(c)], we can see the zero-magnetization plateau with $\tilde{M} = 1$ edge states corresponding to the Haldane gap between $\tilde{M} = 1$ and 2. Interestingly, with applying a small real magnetic field in Fig. 3(d), a quasi-plateau with a small tilt appears in both the real magnetization M and chirality M' . The expectation value of real magnetization $M \cong 1/2$ is composed of two decoupled edge states like Fig. 3(b). Thus, the quarter-spin magnetization can be observed at the edges even with a real magnetic field.

Lastly, we comment on a possibility of experimental setup of the TST model. In our model, the Heisenberg terms in a TST, i.e., $\mathcal{H}_J^{(j)}$ and $\mathcal{H}_{J'}^{(j)}$, are familiar in many quantum spin materials. Hence, the coupling term of the real spin and the chirality $\mathcal{H}_K^{(j)}$ is only distinct in light of real compounds. To understand this term in detail, we rewrite it in original spin operators, leading to

$$S_{\text{tot},j}^z \chi_j^z = \frac{1}{4\sqrt{3}} \sum_{i,i',i''} \epsilon_{ii'i''} (\mathbf{S}_{i',j} \times \mathbf{S}_{i'',j})^z, \quad (13)$$

$$S_{\text{tot},j}^+ \chi_j^- + \text{H.c.} = -\mathcal{P}_j^d (S_{1,j}^x + S_{2,j}^- + S_{3,j}^+) \mathcal{P}_j^d. \quad (14)$$

Here, we use the projection operator into the cluster's doublets $\mathcal{P}_j^d = (15/4 - \mathbf{S}_{\text{tot},j}^2)/3$ and ϕ component of spin $S_{i,j}^{\pm\phi} = (e^{\mp i\phi} S_{i,j}^+ + e^{\pm i\phi} S_{i,j}^-)/2$ with $\phi = 2\pi/3$. Apparently, the Ising part of this interaction (13) corresponds to z component of the vector chirality. Meanwhile, the XY part (14) is regarded as a transverse herical magnetic field with the projection into doublets in a cluster. The projection can be effectively introduced at low temperatures if we consider the case $J \gg K$, although the triplet is slightly broken with a small energy gap $\varepsilon \sim K^2/J$ due to the hybridization effects of the quartet and doublets in a cluster. Note that in this case, the intra-cluster interactions need to be approximately greater than the energy gap $J'_k \gtrsim K^2/J$, to exhibit the CBHS. Therefore, this term may be found in a chiral magnet holding a vector chirality, with applied the transverse herical magnetic field at low temperatures.

In conclusion, we have proposed an exotic extension of the Haldane state to show a novel mechanism of fractionalization of edge states. In this model, the chirality degree of freedom is regarded as an $S = 1/2$ pseudo spin. The real and pseudo spins are symmetrized in the Haldane state of our model, so that an $S = 1/2$ spin degree of freedom appearing as the edge states consists of the real and pseudo spin components. Since the magnetic field is directly coupled with only the real spin, we can observe a half of the magnitude of edge states, corresponding to a quarter spin. Our concept not only gives a new quantum spin feature, but also implies various possibilities of quantum fractionalization.

ACKNOWLEDGMENTS

We would like to thank M. Fujihala, S. Mitsuda, and K. Morita for giving us a motivation of this study through the preceding studies of Fedotovite and a Kagome strip. This work was partly supported by a Grant-in-Aid for Young Scientists (B) (Grant No. 16K17753), Grant-in-Aid for Scientific Research (C) (Grant No. 20K03840). Numerical computation in this work was carried out on the supercomputers at JAEA and the Supercomputer Center at the Institute for Solid State Physics, University of Tokyo.

Appendix A: Derivation the effective Hamiltonian

In this section, we show an explicit derivation of the effective Hamiltonian from the original Hamiltonian of a triangular spin tube:

$$\mathcal{H}_0 = \sum_{j=1}^L \mathcal{H}_J^{(j)} + \sum_{j=1}^{L-1} \mathcal{H}_{J'}^{(j)} + \sum_{j=1}^L \mathcal{H}_K^{(j)} \quad (\text{A1})$$

with

$$\mathcal{H}_J^{(j)} = J \sum_{i < i'} \mathbf{S}_{i,j} \cdot \mathbf{S}_{i',j}, \quad (\text{A2})$$

$$\mathcal{H}_{J'}^{(j)} = J'_1 \sum_i \mathbf{S}_{i,j} \cdot \mathbf{S}_{i,j+1} + J'_2 \sum_{i \neq i'} \mathbf{S}_{i,j} \cdot \mathbf{S}_{i',j+1}, \quad (\text{A3})$$

$$\mathcal{H}_K^{(j)} = -K \mathbf{S}_{\text{tot},j} \cdot \boldsymbol{\chi}_j, \quad (\text{A4})$$

where L is the number of clusters. The local Hamiltonians, $\mathcal{H}_J^{(j)}$, $\mathcal{H}_{J'}^{(j)}$, and $\mathcal{H}_K^{(j)}$, represent intra-cluster spin interactions of the j -th cluster, inter-cluster spin interactions between the j -th and $(j+1)$ -th clusters, and a spin-chirality interaction of the j -th cluster, respectively. The $S = 1/2$ local spin (the total spin) operator in a cluster is denoted by $\mathbf{S}_{i,j}$ ($\mathbf{S}_{\text{tot},j} = \sum_i \mathbf{S}_{i,j}$), where $i = 1, 2, 3$ ($j = 1, 2, \dots, L$) denotes the site (cluster) index. The $S = 1/2$ pseudo spin operator $\boldsymbol{\chi}_j = (\chi_j^x, \chi_j^y, \chi_j^z)$ based on the scalar chirality $\chi_j \equiv (4/\sqrt{3})\mathbf{S}_{1,j} \cdot \mathbf{S}_{2,j} \times \mathbf{S}_{3,j}$ is defined by,

$$\chi_j^x = (\chi_j^+ + \chi_j^-)/2, \quad \chi_j^y = (\chi_j^+ - \chi_j^-)/(2i), \quad \chi_j^z = \chi_j/2 \quad (\text{A5})$$

with the chirality ladder operators $\chi_j^\pm \equiv \sum_{\sigma=\pm\frac{1}{2}} |\sigma, \pm 1\rangle_j \langle \sigma, \mp 1|_j$ and the imaginary unit $i = \sqrt{-1}$. Here, $|\sigma, c\rangle$ ($\sigma = \pm 1/2$ and $c = \pm 1$) represents the simultaneous eigenstates of the total spin $S_{\text{tot},j}^z$ and the scalar chirality.

The triplet ground states with $J > 0$ and $K > 0$ in the cluster Hamiltonians (A2) and (A4) are given by,

$$|\widetilde{1}\rangle_j = \frac{1}{\sqrt{3}} \left(e^{-i\phi} |\uparrow\uparrow\downarrow\rangle_j + e^{i\phi} |\uparrow\downarrow\uparrow\rangle_j + |\downarrow\uparrow\uparrow\rangle_j \right), \quad (\text{A6})$$

$$|\widetilde{0}\rangle_j = \frac{1}{\sqrt{6}} \left(e^{i\phi} |\uparrow\uparrow\downarrow\rangle_j + e^{-i\phi} |\uparrow\downarrow\uparrow\rangle_j + |\downarrow\uparrow\uparrow\rangle_j \right. \\ \left. - e^{-i\phi} |\downarrow\downarrow\uparrow\rangle_j - e^{i\phi} |\downarrow\uparrow\downarrow\rangle_j - |\uparrow\downarrow\downarrow\rangle_j \right), \quad (\text{A7})$$

$$|\widetilde{-1}\rangle_j = -\frac{1}{\sqrt{3}} \left(e^{i\phi} |\downarrow\downarrow\uparrow\rangle_j + e^{-i\phi} |\downarrow\uparrow\downarrow\rangle_j + |\uparrow\downarrow\downarrow\rangle_j \right), \quad (\text{A8})$$

with $\phi = 2\pi/3$. The ket states in the right-hand side denote the direct products of one-spin eigenstates, e.g., $|\uparrow\downarrow\uparrow\rangle_j = |\uparrow\rangle_{1,j} |\downarrow\rangle_{2,j} |\uparrow\rangle_{3,j}$. By using the triplet states, the projection operator is defined by $\mathcal{P}_j = \sum_{m=0,\pm 1} |\widetilde{m}\rangle_j \langle \widetilde{m}|_j$.

At low temperatures $T \ll J, K$, the low-energy physics is well described by the triplet states, neglecting the other states of cluster. Since the triplet states correspond to the eigenstates of an $S = 1$ spin, we can write projected operators of the local spins with the $S = 1$ pseudo spin operator $\widetilde{\mathbf{S}}_j$,

$$\mathcal{P}_j \mathbf{S}_{1,j} \mathcal{P}_j = \mathcal{P}_j \begin{pmatrix} S_{1,j}^x \\ S_{1,j}^y \\ S_{1,j}^z \end{pmatrix} \mathcal{P}_j = \frac{1}{3} \begin{pmatrix} \widetilde{S}_j^x - (\widetilde{S}_j^+)^2 - (\widetilde{S}_j^-)^2 + 2(\widetilde{S}_j^z)^2 - 2 \\ \widetilde{S}_j^y + i(\widetilde{S}_j^+)^2 - i(\widetilde{S}_j^-)^2 \\ \widetilde{S}_j^z - \widetilde{S}_j^z \widetilde{S}_j^+ - \widetilde{S}_j^z \widetilde{S}_j^- - \widetilde{S}_j^+ \widetilde{S}_j^z - \widetilde{S}_j^- \widetilde{S}_j^z \end{pmatrix}, \quad (\text{A9})$$

$$\mathcal{P}_j \mathbf{S}_{2,j} \mathcal{P}_j = \mathcal{P}_j \begin{pmatrix} S_{2,j}^x \\ S_{2,j}^y \\ S_{2,j}^z \end{pmatrix} \mathcal{P}_j = \frac{1}{3} \begin{pmatrix} \widetilde{S}_j^x - e^{i\phi} (\widetilde{S}_j^+)^2 - e^{-i\phi} (\widetilde{S}_j^-)^2 - (\widetilde{S}_j^z)^2 + 1 \\ \widetilde{S}_j^y - e^{i\phi/4} (\widetilde{S}_j^+)^2 - e^{-i\phi/4} (\widetilde{S}_j^-)^2 - \sqrt{3} (\widetilde{S}_j^z)^2 + \sqrt{3} \\ \widetilde{S}_j^z - e^{i\phi} \widetilde{S}_j^z \widetilde{S}_j^+ - e^{-i\phi} \widetilde{S}_j^z \widetilde{S}_j^- - e^{i\phi} \widetilde{S}_j^+ \widetilde{S}_j^z - e^{-i\phi} \widetilde{S}_j^- \widetilde{S}_j^z \end{pmatrix}, \quad (\text{A10})$$

$$\mathcal{P}_j \mathbf{S}_{3,j} \mathcal{P}_j = \mathcal{P}_j \begin{pmatrix} S_{3,j}^x \\ S_{3,j}^y \\ S_{3,j}^z \end{pmatrix} \mathcal{P}_j = \frac{1}{3} \begin{pmatrix} \widetilde{S}_j^x - e^{-i\phi} (\widetilde{S}_j^+)^2 - e^{i\phi} (\widetilde{S}_j^-)^2 - (\widetilde{S}_j^z)^2 + 1 \\ \widetilde{S}_j^y + e^{-i\phi/4} (\widetilde{S}_j^+)^2 + e^{i\phi/4} (\widetilde{S}_j^-)^2 + \sqrt{3} (\widetilde{S}_j^z)^2 - \sqrt{3} \\ \widetilde{S}_j^z - e^{-i\phi} \widetilde{S}_j^z \widetilde{S}_j^+ - e^{i\phi} \widetilde{S}_j^z \widetilde{S}_j^- - e^{-i\phi} \widetilde{S}_j^+ \widetilde{S}_j^z - e^{i\phi} \widetilde{S}_j^- \widetilde{S}_j^z \end{pmatrix}. \quad (\text{A11})$$

Although it is not so easy to calculate the inter-cluster interactions step by step with these operators, the total spin has a simple form $\mathcal{P}_j \mathbf{S}_{\text{tot},j} \mathcal{P}_j = \widetilde{\mathbf{S}}_j$. Therefore, we can easily obtain the effective Hamiltonian of an equiva-

lent case of the inter-cluster interactions $J'_1 = J'_2 (\equiv J')$,

$$\mathcal{H}_{\text{eff}}^{(j)} |_{J'_1=J'_2=J'} = (\mathcal{P}_j \mathcal{P}_{j+1}) \mathcal{H}_{J'}^{(j)} |_{J'_1=J'_2} (\mathcal{P}_j \mathcal{P}_{j+1}) \\ = J' (\mathcal{P}_j \mathcal{P}_{j+1}) (\mathbf{S}_{\text{tot},j} \cdot \mathbf{S}_{\text{tot},j+1}) (\mathcal{P}_j \mathcal{P}_{j+1}) = J' \widetilde{\mathbf{S}}_j \cdot \widetilde{\mathbf{S}}_{j+1}. \quad (\text{A12})$$

On the other hand, though a discord case $J'_1 \neq J'_2$ is not so easy, the case of $J'_2 = 0$ is relatively easy to ob-

tain. Moreover, if the effective Hamiltonian of (i) $J'_1 \neq 0$ and $J'_2 = 0$ is obtained, we can also obtain the effective Hamiltonian for (ii) $J'_1 = 0$ and $J'_2 \neq 0$, because the equivalent case of effective Hamiltonian (A12) is the sum of both the cases,

$$\mathcal{H}_{\text{eff}}^{(j)}|_{J'_1=J'_2=J'} = \mathcal{H}_{\text{eff}}^{(j)}|_{J'_1=J' \neq 0, J'_2=0} + \mathcal{H}_{\text{eff}}^{(j)}|_{J'_1=0, J'_2=J' \neq 0}. \quad (\text{A13})$$

Then, to obtain the effective Hamiltonian in general case, it is sufficient to show the case of (i) $J'_1 \neq 0$ and $J'_2 = 0$. With the relation $\sum_i \left(\mathcal{P}_j \mathbf{S}_{i,j} \mathcal{P}_j - \frac{1}{3} \tilde{\mathbf{S}}_j \right) = 0$, the effective Hamiltonian of the J'_1 term is rewritten by,

$$\begin{aligned} \mathcal{H}_{\text{eff}}^{(j)}|_{J'_1 \neq 0, J'_2 = 0} &= J'_1 \sum_{\alpha, i} (\mathcal{P}_j \mathcal{P}_{j+1}) (S_{i,j}^\alpha S_{i,j+1}^\alpha) (\mathcal{P}_j \mathcal{P}_{j+1}) \\ &= J'_1 \sum_{\alpha, i} \left[\left(\mathcal{P}_j S_{i,j}^\alpha \mathcal{P}_j - \frac{1}{3} \tilde{S}_j^\alpha \right) + \frac{1}{3} \tilde{S}_j^\alpha \right] \left[\left(\mathcal{P}_{j+1} S_{i,j+1}^\alpha \mathcal{P}_{j+1} - \frac{1}{3} \tilde{S}_{j+1}^\alpha \right) + \frac{1}{3} \tilde{S}_{j+1}^\alpha \right] \\ &= \frac{J'_1}{3} \tilde{\mathbf{S}}_j \cdot \tilde{\mathbf{S}}_{j+1} + J'_1 \sum_{\alpha, i} \left(\mathcal{P}_j S_{i,j}^\alpha \mathcal{P}_j - \frac{1}{3} \tilde{S}_j^\alpha \right) \left(\mathcal{P}_{j+1} S_{i,j+1}^\alpha \mathcal{P}_{j+1} - \frac{1}{3} \tilde{S}_{j+1}^\alpha \right). \end{aligned} \quad (\text{A14})$$

According to (A9)–(A11), we can rewrite the second term into

$$\begin{aligned} &\sum_{\alpha, i} \left(\mathcal{P}_j S_{i,j}^\alpha \mathcal{P}_j - \frac{1}{3} \tilde{S}_j^\alpha \right) \left(\mathcal{P}_{j+1} S_{i,j+1}^\alpha \mathcal{P}_{j+1} - \frac{1}{3} \tilde{S}_{j+1}^\alpha \right) \\ &= \frac{1}{9} \sum_{\alpha, i} \sum_{m, n} (a_{i,m}^\alpha O_{j,m}^\alpha) (a_{i,n}^\alpha O_{j+1,n}^\alpha) \\ &= \frac{1}{9} \sum_{\alpha} \sum_{m, n} O_{j,m}^\alpha \left(\sum_i a_{i,m}^\alpha a_{i,n}^\alpha \right) O_{j+1,n}^\alpha, \end{aligned} \quad (\text{A15})$$

with coefficient and operator vectors, $\mathbf{a}_i^\alpha = \{a_{i,m}^\alpha\}$ and $\mathbf{O}_j^\alpha = \{O_{j,m}^\alpha\}$ ($m = 1, 2, 3, 4$) given by,

$$\mathbf{a}_1^x = -(1, 1, -2, 2), \quad (\text{A16})$$

$$\mathbf{a}_2^x = -(e^{i\phi}, e^{-i\phi}, 1, -1), \quad (\text{A17})$$

$$\mathbf{a}_3^x = -(e^{-i\phi}, e^{i\phi}, 1, -1), \quad (\text{A18})$$

$$\mathbf{a}_1^y = (i, -i, 0, 0), \quad (\text{A19})$$

$$\mathbf{a}_2^y = -(e^{i\phi/4}, e^{-i\phi/4}, \sqrt{3}, -\sqrt{3}), \quad (\text{A20})$$

$$\mathbf{a}_3^y = (e^{-i\phi/4}, e^{i\phi/4}, \sqrt{3}, -\sqrt{3}), \quad (\text{A21})$$

$$\mathbf{a}_1^z = -(1, 1, 1, 1), \quad (\text{A22})$$

$$\mathbf{a}_2^z = -(e^{i\phi}, e^{-i\phi}, e^{i\phi}, e^{-i\phi}), \quad (\text{A23})$$

$$\mathbf{a}_3^z = -(e^{-i\phi}, e^{i\phi}, e^{-i\phi}, e^{i\phi}), \quad (\text{A24})$$

and

$$\mathbf{O}_j^x = \mathbf{O}_j^y = \left((\tilde{S}_j^+)^2, (\tilde{S}_j^-)^2, (\tilde{S}_j^z)^2, 1 \right), \quad (\text{A25})$$

$$\mathbf{O}_j^z = \left(\tilde{S}_j^z \tilde{S}_j^+, \tilde{S}_j^z \tilde{S}_j^-, \tilde{S}_j^+ \tilde{S}_j^z, \tilde{S}_j^- \tilde{S}_j^z \right). \quad (\text{A26})$$

The coefficient matrices in (A15) are obtained as the direct product of the coefficient vectors,

$$\mathbf{A}_i^\alpha = \{(A_i^\alpha)_{m,n}\} = \{a_{i,m}^\alpha a_{i,n}^\alpha\} = \mathbf{a}_i^\alpha \otimes \mathbf{a}_i^\alpha. \quad (\text{A27})$$

The sum of the coefficient matrices $\mathbf{A}_{\text{tot}}^\alpha = \sum_i \mathbf{A}_i^\alpha$ is easily calculated, leading to

$$\mathbf{A}_{\text{tot}}^x = \begin{pmatrix} 0 & 3 & -3 & 3 \\ 3 & 0 & -3 & 3 \\ -3 & -3 & 6 & -6 \\ 3 & 3 & -6 & 6 \end{pmatrix}, \quad (\text{A28})$$

$$\mathbf{A}_{\text{tot}}^y = \begin{pmatrix} 0 & 3 & 3 & -3 \\ 3 & 0 & 3 & -3 \\ 3 & 3 & 6 & -6 \\ -3 & -3 & -6 & 6 \end{pmatrix}, \quad (\text{A29})$$

$$\mathbf{A}_{\text{tot}}^z = \begin{pmatrix} 0 & 3 & 0 & 3 \\ 3 & 0 & 3 & 0 \\ 0 & 3 & 0 & 3 \\ 3 & 0 & 3 & 0 \end{pmatrix}. \quad (\text{A30})$$

With these matrices, we can rewrite (A15) into

$$\begin{aligned} &\sum_{\alpha, i} \left(\mathcal{P}_j S_{i,j}^\alpha \mathcal{P}_j - \frac{1}{3} \tilde{S}_j^\alpha \right) \left(\mathcal{P}_{j+1} S_{i,j+1}^\alpha \mathcal{P}_{j+1} - \frac{1}{3} \tilde{S}_{j+1}^\alpha \right) \\ &= \frac{J'_1}{9} [\mathbf{O}_j^x (\mathbf{A}_{\text{tot}}^x + \mathbf{A}_{\text{tot}}^y) (\mathbf{O}_j^x)^T + \mathbf{O}_j^z \mathbf{A}_{\text{tot}}^z (\mathbf{O}_j^z)^T]. \end{aligned} \quad (\text{A31})$$

Calculating the vector-matrix-vector products in the right-hand side, we finally obtain the effective Hamiltonian of (i) $J'_1 \neq 0$ and $J'_2 = 0$ as follows,

$$\mathcal{H}_{\text{eff}}^{(j)}|_{J'_1 \neq 0, J'_2 = 0} = J'_1 \left\{ \left(\frac{5}{3} \tilde{S}_j^z \tilde{S}_{j+1}^z + \tilde{S}_j^x \tilde{S}_{j+1}^x + \tilde{S}_j^y \tilde{S}_{j+1}^y \right) + \frac{8}{3} \left(\frac{1}{2} \tilde{S}_j^z \tilde{S}_{j+1}^z + \tilde{S}_j^x \tilde{S}_{j+1}^x + \tilde{S}_j^y \tilde{S}_{j+1}^y \right) \right. \\ \left. - \frac{2}{3} \left[2 - (\tilde{S}_j^z)^s \right] \left[2 - (\tilde{S}_{j+1}^z)^s \right] - \frac{4}{3} \right\}. \quad (\text{A32})$$

Thus, the effective Hamiltonian of (ii) $J'_1 = 0$ and $J'_2 \neq 0$ is obtained by,

$$\mathcal{H}_{\text{eff}}^{(j)}|_{J'_1 = 0, J'_2 \neq 0} = \frac{J'_2}{J'} \left(\mathcal{H}_{\text{eff}}^{(j)}|_{J'_1 \rightarrow J', J'_2 \rightarrow J'} - \mathcal{H}_{\text{eff}}^{(j)}|_{J'_1 \rightarrow J', J'_2 = 0} \right) \\ = -J'_2 \left\{ \frac{2}{3} \tilde{S}_j^z \tilde{S}_{j+1}^z + \frac{8}{3} \left(\frac{1}{2} \tilde{S}_j^z \tilde{S}_{j+1}^z - \tilde{S}_j^x \tilde{S}_{j+1}^x + \tilde{S}_j^y \tilde{S}_{j+1}^y \right) + \frac{2}{3} \left[2 - (\tilde{S}_j^z)^s \right] \left[2 - (\tilde{S}_{j+1}^z)^s \right] - \frac{4}{3} \right\}. \quad (\text{A33})$$

We have also confirmed the derivation of effective Hamiltonians from the original Hamiltonians with the matrix form in the two-cluster Hilbert spaces, corresponding to the projection of $(2^3)^2 \times (2^3)^2$ matrices to $3^2 \times 3^2$ matrices.

in the variational matrix-product state (VMPS) method. For simplicity, we firstly divide the Hamiltonian (A1) into two-body terms preserving the magnetization and three-body terms (including one-body terms) breaking the magnetization,

Appendix B: Matrix-product operator representations of the Hamiltonian

$$\mathcal{H}_0 = \mathcal{H}_{2b} + \mathcal{H}_{3b} \quad (\text{B1})$$

In this section, we show the matrix-product operator (MPO) representation of the Hamiltonian, which is used

with

$$\mathcal{H}_{2b} = \sum_{j=1}^L \mathcal{H}_j^{(j)} + \sum_{j=1}^{L-1} \mathcal{H}_{j'}^{(j)} - K \sum_{j=1}^L S_{\text{tot},j}^z \chi_j^z \\ = J \sum_{j=1}^L \sum_{i < i'} \mathbf{S}_{i,j} \cdot \mathbf{S}_{i',j} + J'_1 \sum_{j=1}^{L-1} \sum_i \mathbf{S}_{i,j} \cdot \mathbf{S}_{i,j+1} + J'_2 \sum_{j=1}^{L-1} \sum_{i \neq i'} \mathbf{S}_{i,j} \cdot \mathbf{S}_{i',j+1} - \frac{K}{4\sqrt{3}} \sum_{j=1}^L \sum_{i,i',i''} \epsilon_{ii'i''} (\mathbf{S}_{i',j} \times \mathbf{S}_{i'',j})^z \quad (\text{B2})$$

$$\mathcal{H}_{3b} = -\frac{K}{2} \sum_{j=1}^L (S_{\text{tot},j}^+ \chi_j^- + S_{\text{tot},j}^- \chi_j^+) = -\frac{2K}{3} \sum_{j=1}^L \left[S_1^x \text{Hs}_j(2, 3) + S_2^\phi \text{Hs}_j(3, 1) + S_3^{-\phi} \text{Hs}_j(1, 2) \right]. \quad (\text{B3})$$

Here, we use the energy-shifted Heisenberg interaction in the j -th cluster $\text{Hs}_j(i, i') = \mathbf{S}_{i,j} \cdot \mathbf{S}_{i',j} - 1/4$, and ϕ component of spin $S_{i,j}^{\pm\phi} = (e^{\mp i\phi} S_{i,j}^+ + e^{\pm i\phi} S_{i,j}^-)/2$ with $\phi = 2\pi/3$.

According to a review of the VMPS method [47], the MPO representation of two-body terms are easily obtained as follows,

$$\mathcal{H}_{2b} = \mathbf{H}_1 \mathbf{H}_2 \cdots \mathbf{H}_{N-1} \mathbf{H}_N^T, \quad (\text{B4})$$

where the local matrix or vector operators are given by,

$$\mathbf{H}_1 = (0, \mathbf{P}_1, \mathbf{M}_1, \mathbf{Z}_1, 1), \quad (\text{B5})$$

$$\mathbf{H}_j = \begin{pmatrix} 1 & & & & \\ \mathbf{m}_j^T & \mathbf{L} & & & \\ \mathbf{p}_j^T & & \mathbf{L} & & \\ \mathbf{z}_j^T & & & \mathbf{L} & \\ 0 & \mathbf{P}_j & \mathbf{M}_j & \mathbf{Z}_j & 1 \end{pmatrix} \quad (j = 2, 3, \dots, N-1), \quad (\text{B6})$$

$$\mathbf{H}_N = (1, \mathbf{m}_N, \mathbf{p}_N, \mathbf{z}_N, 0), \quad (\text{B7})$$

with the lower matrix

$$\mathbf{L} = \begin{pmatrix} 0 & 0 & 0 & 0 & 0 \\ 1 & 0 & 0 & 0 & 0 \\ 0 & 1 & 0 & 0 & 0 \\ 0 & 0 & 1 & 0 & 0 \\ 0 & 0 & 0 & 1 & 0 \end{pmatrix}. \quad (\text{B8})$$

Here, we define local vector operators in the dimension of energy for $j = 0, 1, 2 \pmod{3}$ as follows.

- $j = 0 \pmod{3}$

$$\mathbf{P}_j = \frac{1}{2} (J'_2, J'_2, J'_1, 0, 0) S_j^+, \quad (\text{B9})$$

$$\mathbf{M}_j = \frac{1}{2} (J'_2, J'_2, J'_1, 0, 0) S_j^-, \quad (\text{B10})$$

$$\mathbf{Z}_j = (J'_2, J'_2, J'_1, 0, 0) S_j^z. \quad (\text{B11})$$

- $j = 1 \pmod{3}$

$$\mathbf{P}_j = \frac{1}{2} (J - \iota K/(4\sqrt{3}), J + \iota K/(4\sqrt{3}), J'_1, J'_2, J'_2) S_j^+, \quad (\text{B12})$$

$$\mathbf{M}_j = \frac{1}{2} (J + \iota K/(4\sqrt{3}), J - \iota K/(4\sqrt{3}), J'_1, J'_2, J'_2) S_j^-, \quad (\text{B13})$$

$$\mathbf{Z}_j = (J, J, J'_1, J'_2, J'_2) S_j^z. \quad (\text{B14})$$

- $j = 2 \pmod{3}$

$$\mathbf{P}_j = \frac{1}{2} (J - \iota K/(4\sqrt{3}), J'_2, J'_1, J'_2, 0) S_j^+, \quad (\text{B15})$$

$$\mathbf{M}_j = \frac{1}{2} (J + \iota K/(4\sqrt{3}), J'_2, J'_1, J'_2, 0) S_j^-, \quad (\text{B16})$$

$$\mathbf{Z}_j = (J, J'_2, J'_1, J'_2, 0) S_j^z. \quad (\text{B17})$$

The dimensionless local vector operators are defined by,

$$\mathbf{p}_j = (S_j^+, 0, 0, 0, 0), \quad (\text{B18})$$

$$\mathbf{m}_j = (S_j^-, 0, 0, 0, 0), \quad (\text{B19})$$

$$\mathbf{z}_j = (S_j^z, 0, 0, 0, 0). \quad (\text{B20})$$

On the other hand, the MPO representation of the three-body terms is neither trivial nor unique. We use the following form of the MPO representation.

$$\mathcal{H}_{3b} = \mathbf{V}_1 \mathbf{V}_2 \cdots \mathbf{V}_{N-1} \mathbf{V}_N^T, \quad (\text{B21})$$

where the local vector operators at edge sites are given by,

$$\mathbf{V}_1 = (\mathbf{v}_1, -(2/3) K S_1^x, 0, 1), \quad (\text{B22})$$

$$\mathbf{V}_N = (\mathbf{v}_N, -(2/3) K S_N^{-\phi}, 1, 0), \quad (\text{B23})$$

with

$$\mathbf{v}_j = (S_j^x, S_j^y, S_j^z, \iota/2). \quad (\text{B24})$$

The local matrix operators for $j = 2, 3, \dots, N-1$ are defined by the following three forms depending on the site index j .

- $j = 0 \pmod{3}$

$$\mathbf{V}_j = \begin{pmatrix} \mathbf{v}_j & -(2/3) K S_j^{-\phi} & 1 & 0 \\ \mathbf{0} & 0 & 0 & 1 \end{pmatrix}^T. \quad (\text{B25})$$

- $j = 1 \pmod{3}$

$$\mathbf{V}_j = \begin{pmatrix} \mathbf{0} & 0 & 1 & 0 \\ \mathbf{v}_j & -(2/3) K S_j^x & 0 & 1 \end{pmatrix}. \quad (\text{B26})$$

- $j = 2 \pmod{3}$

$$\mathbf{V}_j = \left(\begin{array}{c|c} -(2/3) K S_j^\phi \mathbf{1}_4 & \mathbf{v}_j^T \\ \hline \mathbf{v}_j & 0 \end{array} \middle| \mathbf{1}_2 \right), \quad (\text{B27})$$

where $\mathbf{1}_4$ ($\mathbf{1}_2$) denotes the 4×4 (2×2) identity matrix.

Note that the MPO representation of a cluster given by a product of three local matrix operators $V_j V_{j+1} V_{j+2}$ for $j = 1 \pmod{3}$ except for $j = 1$ and $N-2$ as follows,

$$V_j V_{j+1} V_{j+2} = \begin{pmatrix} 1 & 0 \\ \mathcal{H}_{3b}^{(j)} & 1 \end{pmatrix} \quad (\text{B28})$$

with

$$\mathcal{H}_{3b}^{(j)} = -\frac{2K}{3} \left[S_1^x \text{Hs}_j(2, 3) + S_2^\phi \text{Hs}_j(3, 1) + S_3^{-\phi} \text{Hs}_j(1, 2) \right]. \quad (\text{B29})$$

By using this form, we can easily confirm the correspondence of the three-body Hamiltonian (B3) and its MPO representation (B21).

[1] P. A. M. Dirac, Quantised Singularities in Electromagnetic Field, Proc. Roy. Soc. **A133**, 60 (1931).
 [2] P. A. Dirac, The theory of magnetic poles, Phys. Rev. **74**, 817 (1948).
 [3] F. Wilczek, Two applications of axion electrodynamics, Phys. Rev. Lett. **58**, 1799 (1987).

[4] G. Bertone and D. Hooper, History of dark matter, Rev. Mod. Phys. **90**, 045002 (2018).
 [5] P. A. Lee, N. Nagaosa, and X. G. Wen, Doping a Mott insulator: Physics of high-temperature superconductivity, Rev. Mod. Phys. **78**, 17 (2006).
 [6] H. L. Stormer, Fractional quantum hall effect today, Rev.

- Mod. Phys. **71**, S298 (1999).
- [7] G. Murthy and R. Shankar, Hamiltonian theories of the fractional quantum Hall effect, Rev. Mod. Phys. **75**, 1101 (2003).
- [8] X. L. Qi and S. C. Zhang, Topological insulators and superconductors, Rev. Mod. Phys. **83**, 1057 (2011).
- [9] F. D. M. Haldane, Nonlinear field theory of large-spin Heisenberg antiferromagnets: Semiclassically quantized solitons of the one-dimensional easy-axis Néel state, Phys. Rev. Lett. **50**, 1153 (1983).
- [10] F. D. M. Haldane, Nobel lecture: Topological quantum matter, Rev. Mod. Phys. **89**, 040502 (2017).
- [11] A. Kitaev, Anyons in an exactly solved model and beyond, Ann. Phys. (N. Y.) **321**, 2 (2006).
- [12] F. Pollmann, A. M. Turner, E. Berg, and M. Oshikawa, Entanglement spectrum of a topological phase in one dimension, Phys. Rev. B **81**, 064439 (2010).
- [13] X. Chen, Z. C. Gu, and X. G. Wen, Complete classification of one-dimensional gapped quantum phases in interacting spin systems, Phys. Rev. B **84**, 235128 (2011).
- [14] F. Pollmann, E. Berg, A. M. Turner, and M. Oshikawa, Symmetry protection of topological phases in one-dimensional quantum spin systems, Phys. Rev. B **85**, 075125 (2012).
- [15] X. Chen, Z. C. Gu, Z. X. Liu, and X. G. Wen, Symmetry-protected topological orders in interacting bosonic systems, Science **338**, 1604 (2012).
- [16] D. Gross and J. Eisert, Novel schemes for measurement-based quantum computation, Phys. Rev. Lett. **98**, 220503 (2007).
- [17] G. K. Brennen and A. Miyake, Measurement-based quantum computer in the gapped ground state of a two-body hamiltonian, Phys. Rev. Lett. **101**, 010502 (2008).
- [18] A. Miyake, Quantum computation on the edge of a symmetry-protected topological order, Phys. Rev. Lett. **105**, 040501 (2010).
- [19] S. D. Bartlett, G. K. Brennen, A. Miyake, and J. M. Renes, Quantum computational renormalization in the haldane phase, Phys. Rev. Lett. **105**, 110502 (2010).
- [20] D. V. Else, I. Schwarz, S. D. Bartlett, and A. C. Doherty, Symmetry-protected phases for measurement-based quantum computation, Phys. Rev. Lett. **108**, 240505 (2012).
- [21] I. Affleck, T. Kennedy, E. H. Lieb, and H. Tasaki, Valence bond ground states in isotropic quantum antiferromagnets, Commun. Math. Phys. **115**, 477 (1988).
- [22] M. den Nijs and K. Rommelse, Preroughening transitions in crystal surfaces and valence-bond phases in quantum spin chains, Phys. Rev. B **40**, 4709 (1989).
- [23] H. Tasaki, Quantum liquid in antiferromagnetic chains: A stochastic geometric approach to the Haldane gap, Phys. Rev. Lett. **66**, 798 (1991).
- [24] T. Kennedy and H. Tasaki, Hidden $Z_2 \times Z_2$ symmetry breaking in Haldane-gap antiferromagnets, Phys. Rev. B **45**, 304 (1992).
- [25] T. Masuda, A. Zheludev, H. Manaka, L. P. Regnault, J. H. Chung, and Y. Qiu, Dynamics of composite haldane spin chains in IPA-CuCl₃, Phys. Rev. Lett. **96**, 047210 (2006).
- [26] M. Fujihala, T. Sugimoto, T. Tohyama, S. Mitsuda, R. A. Mole, D. H. Yu, S. Yano, Y. Inagaki, H. Morodomi, T. Kawae, H. Sagayama, R. Kumai, Y. Murakami, K. Tomiyasu, A. Matsuo, and K. Kindo, Cluster-Based Haldane State in an Edge-Shared Tetrahedral Spin-Cluster Chain: Fedotovite K₂Cu₃O(SO₄)₃, Phys. Rev. Lett. **120**, 077201 (2018).
- [27] T. Sugimoto, K. Morita, and T. Tohyama, Cluster-based Haldane states in spin-1/2 cluster chains, Phys. Rev. Res. **2**, 023420 (2020).
- [28] K. Kawano and M. Takahashi, Three-leg antiferromagnetic Heisenberg Ladder with frustrated boundary condition; Ground state properties, J. Phys. Soc. Jpn. **66**, 4001 (1997).
- [29] A. Lüscher, R. M. Noack, G. Misguich, V. N. Kotov, and F. Mila, Soliton binding and low-lying singlets in frustrated odd-legged S=1/2 spin tubes, Phys. Rev. B **70**, 060405(R) (2004).
- [30] K. Okunishi, S. I. Yoshikawa, T. Sakai, and S. Miyashita, Low-energy excitations of the S = 1/2 quantum spin tube with the triangular lattice structure, Prog. Theor. Phys. Suppl. **159**, 297 (2005).
- [31] J. B. Fouet, A. Läuchli, S. Pilgram, R. M. Noack, and F. Mila, Frustrated three-leg spin tubes: From spin 1 2 with chirality to spin 3 2, Phys. Rev. B **73**, 014409 (2006).
- [32] M. Sato and T. Sakai, Vector chirality and inhomogeneous magnetization in frustrated spin tubes in high magnetic fields, Phys. Rev. B **75**, 014411 (2007).
- [33] S. Nishimoto and M. Arikawa, Low-lying excitations of the three-leg spin tube: A density-matrix renormalization group study, Phys. Rev. B **78**, 054421 (2008).
- [34] T. Sakai, M. Sato, K. Okunishi, Y. Otsuka, K. Okamoto, and C. Itoi, Quantum phase transitions of the asymmetric three-leg spin tube, Phys. Rev. B **78**, 184415 (2008).
- [35] D. Charrier, S. Capponi, M. Oshikawa, and P. Pujol, Quantum phase transitions in three-leg spin tubes, Phys. Rev. B **82**, 075108 (2010).
- [36] K. Okamoto, M. Sato, K. Okunishi, T. Sakai, and C. Itoi, Magnetization plateau of the quantum spin nanotube, Phys. E **43**, 769 (2011).
- [37] K. Okunishi, M. Sato, T. Sakai, K. Okamoto, and C. Itoi, Spin-chirality separation and S 3 symmetry breaking in the magnetization plateau of the quantum spin tube, Phys. Rev. B **85**, 054416 (2012).
- [38] Y. Zhao, S. S. Gong, Y. J. Wang, and G. Su, Low-energy effective theory and two distinct critical phases in a spin-12 frustrated three-leg spin tube, Phys. Rev. B **86**, 224406 (2012).
- [39] K. Yonaga and N. Shibata, Ground state phase diagram of twisted three-leg spin tube in magnetic field, J. Phys. Soc. Jpn. **84**, 094706 (2015).
- [40] R. C. Alécio, M. L. Lyra, and J. Strečka, Ground states, magnetization plateaus and bipartite entanglement of frustrated spin-1/2 Ising-Heisenberg and Heisenberg triangular tubes, J. Magn. Magn. Mater. **417**, 294 (2016).
- [41] J. Schnack, H. Nojiri, P. Kögerler, G. J. T. Cooper, and L. Cronin, Magnetic characterization of the frustrated three-leg ladder compound [(CuCl₂tachH)₃Cl]Cl₂, Phys. Rev. B **70**, 174420 (2004).
- [42] H. Manaka, Y. Hirai, Y. Hachigo, M. Mitsunaga, M. Ito, and N. Terada, Spin-liquid state study of equilateral triangle S = 3/2 spin tubes formed in CsCrF₄, J. Phys. Soc. Jpn. **78**, 093701 (2009).
- [43] N. B. Ivanov, J. Schnack, R. Schnalle, J. Richter, P. Kögerler, G. N. Newton, L. Cronin, Y. Oshima, and H. Nojiri, Heat capacity reveals the physics of a frustrated spin tube, Phys. Rev. Lett. **105**, 037206 (2010).
- [44] H. Manaka, T. Etoh, Y. Honda, N. Iwashita, K. Ogata, N. Terada, T. Hisamatsu, M. Ito, Y. Narumi, A. Kondo,

- K. Kindo, and Y. Miura, Effects of geometrical spin frustration on triangular spin tubes formed in CsCrF_4 and $\alpha\text{-KCrF}_4$, *J. Phys. Soc. Jpn.* **80**, 084714 (2011).
- [45] H. Manaka, H. Morita, T. Akasaka, Y. Miura, M. Hagihala, S. Hayashida, M. Soda, and T. Masuda, Substitution effects on magnetic ground states with geometrical spin frustration in triangular spin tubes formed in CsCrF_4 and $\alpha\text{-KCrF}_4$, *J. Phys. Soc. Jpn.* **88**, 114703 (2019).
- [46] M. Hagihala, S. Hayashida, M. Avdeev, H. Manaka, H. Kikuchi, and T. Masuda, Magnetic states of coupled spin tubes with frustrated geometry in CsCrF_4 , *npj Quantum Mater.* **4**, 14 (2019).
- [47] U. Schollwöck, The density-matrix renormalization group in the age of matrix product states, *Ann. Phys. (N. Y.)* **326**, 96 (2011).